THE JOURNAL OF BIOLOGICAL CHEMISTRY
Vol. 279, No. 23, Issue of June 4, pp. 24387–24393, 2004

Printed in U.S.A.

Mice Lacking Thioredoxin-interacting Protein Provide Evidence Linking Cellular Redox State to Appropriate Response to Nutritional Signals*

Received for publication, February 5, 2004, and in revised form, March 24, 2004
Published, JBC Papers in Press, March 26, 2004, DOI 10.1074/jbc. M401280200

To Yuen Hui‡, Sonal S. Sheth§, J. Matthew Diffley‡, Douglas W. Potter‡, Aldons J. Lusis§, Alan D. Attie¶, and Roger A. Davis‡‖

From the ‡Mammalian Cell and Molecular Biology Laboratory, Department of Biology, Molecular Biology Institute and Heart Institute, San Diego State University, San Diego, California 92182, §Molecular Biology Institute and Department of Medicine, Microbiology and Human Genetics, University of California, Los Angeles, California 90095, and ¶Department of Biochemistry, University of Wisconsin, Madison, Wisconsin 53706

Thioredoxin-interacting protein (Txnip) is a ubiquitous protein that binds with high affinity to thioredoxin and inhibits its ability to reduce sulfhydryl groups via NADPH oxidation. HcB-19 mice contain a nonsense mutation in Txnip that eliminates its expression. Unlike normal animals, HcB-19 mice have ~3-fold increase in insulin levels when fasted. The C-peptide/insulin ratio is normal, suggesting that the hyperinsulinemia is due to increased insulin secretion. Fasted HcB-19 mice are hypoglycemic, hypertriglyceridemic, and have higher than normal levels of ketone bodies. Ablation of pancreatic β-cells with streptozotocin completely blocks the fasting-induced hypoglycemia/hypertriglyceridemia, suggesting that these abnormalities are due to excess insulin secretion. This is supported by increased hepatic mRNA levels of the insulin-inducible, lipogenic transcription factor sterol-responsive element-binding protein-1c and two of its targets, acetyl-CoA carboxylase and fatty acid synthase. During a prolonged fast, the hyperinsulinemia up-regulates lipogenesis but fails to down-regulate hepatic phosphoenolpyruvate carboxykinase mRNA expression. Hepatic ratios of reduced:oxidized glutathione, established regulators of gluconeogenic/glycolytic/lipogenic enzymes, were elevated 30% in HcB-19 mice, suggesting a loss of Txnip-enhanced sulfhydryl reduction. The altered hepatic enzymatic profiles of HcB-19 mice divert phosphoenolpyruvate to glyceroneogenesis and lipogenesis rather than gluconeogenesis. Our findings implicate Txnip-modulated sulfhydryl redox as a central regulator of insulin secretion in β-cells and regulation of many of the branch-points of gluconeogenesis/glycolysis/lipogenesis.

The liver plays a central role in controlling the flow of nutrients to and from peripheral tissues. The flux of carbon units through hepatic pathways of lipid and carbohydrate metabolism are rapidly changed in response to nutrition. In the transition from the fed to the fasted state, hepatocytes switch from being primarily glycolytic and lipogenic to being gluconeogenic and ketogenic. This occurs in response to a drop in blood insulin and to a lesser degree, an increase in glucagon levels.

Lipids are exported by the liver in the form of triglyceride-rich very low density lipoprotein (VLDL)[1] particles. Depending on the metabolic state, there are two major sources of free fatty acids that are channeled into hepatic triglyceride production. In the fed state, hepatocytes up-regulate the expression of glycolytic and lipogenic enzymes, primarily by increasing the expression and activation of a master regulator, the transcription factor SREBP-1c (1). This process converts carbohydrate into fatty acids, which are then esterified to form triglycerides, the major core lipid secreted by the liver as VLDL. In the fasted state, adipose tissue releases free fatty acids from triglyceride stores because insulin levels drop below a threshold required to repress lipolysis and also because of glucagon action. Although the liver does not actively synthesize fatty acids under fasting conditions, it retains the ability to esterify adipose tissue-derived free fatty acids and to export VLDL particles. As much as 50% of fatty acids taken up by the liver during fasting are eventually released as VLDL triglycerides (2). Indeed, in some animal species (*e.g.* ponies), prolonged fasting leads to hypertriglyceridemia (3).

Fasting leads to enhanced gluconeogenesis by the liver. This is largely due to an increase in the expression of key gluconeogenic enzymes, phosphoenolpyruvate carboxykinase (PEPCK) (4), fructose-1,6-bisphosphatase (FBPase) (5), and glucose-6-phosphatase (G6Pase) (6). Thus, there is usually an inverse relationship between gluconeogenesis and lipogenesis in the liver (2, 6, 7).

Hypertriglyceridemia is one of the most common lipid disorders in the human population. It is usually associated with obesity, insulin resistance, and diabetes (8, 9) but is also observed in people without these metabolic disorders (10, 11). There is still a dearth of knowledge about the key genes that contribute to hypertriglyceridemia. However, in the majority of cases, excess triglycerides are derived from overproduction rather than defective catabolism of VLDL (8, 9).

The HcB-19 mouse is a variant of the C3H strain that was

* This project was supported by National Institutes of Health Grant HL51648 (to R. A. D.) and American Heart Association Scientist Development Award 0330109N (to T. Y. H.). The costs of publication of this article were defrayed in part by the payment of page charges. This article must therefore be hereby marked "*advertisement*" in accordance with 18 U.S.C. Section 1734 solely to indicate this fact.

‖ To whom correspondence should be addressed: Mammalian Cell and Molecular Biology Laboratory, Life Sciences Bldg. LS307, 5500 Campanile Dr., San Diego State University, San Diego, CA 92182-4614. Tel.: 619-594-7936. Fax: 619-594-7937; E-mail: rdavis@sunstroke.sdsu.edu.

[1] The abbreviations used are: VLDL, very low density lipoproteins; SREBP, sterol-responsive element-binding protein; FAS, fatty acid synthase; ACC, acetyl-CoA carboxylase; G6P, glucose 6-phosphate; G6Pase, glucose-6-phosphatase; F6P, fructose-6-phosphate; FBPase, fructose-1,6-bisphosphatase; PEPCK, phosphoenolpyruvate carboxykinase; Txnip, thioredoxin-interacting protein; STZ, streptozotocin; DHAP, dihydroxyacetone phosphate.

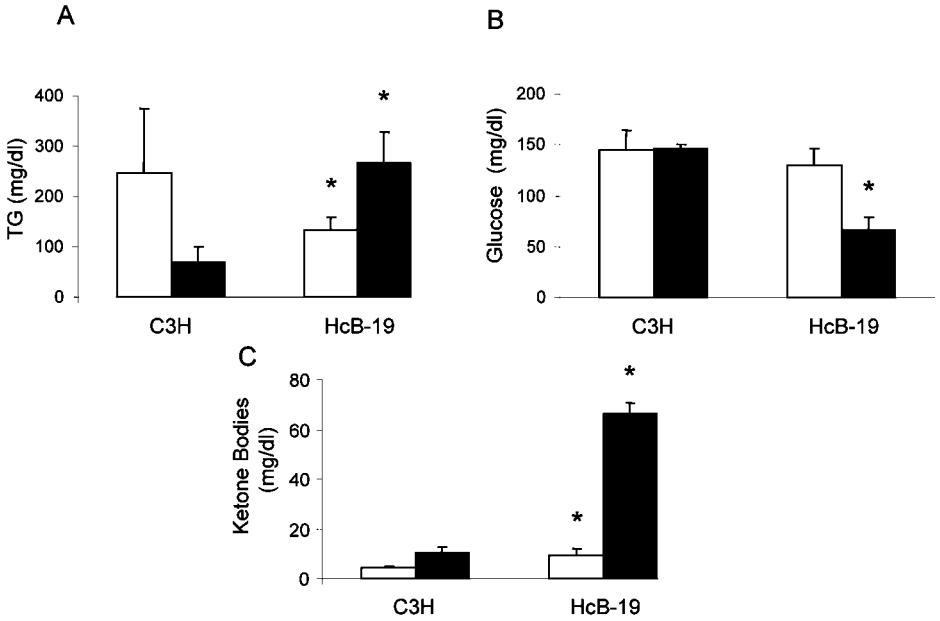

FIG. 1. **Plasma triglyceride (*TG*), glucose, and ketone body levels in HcB-19 and control C3H mice.** C3H (control) and HcB-19 were fed a chow diet and water *ad libitum* in a room with a 12 h light cycle (lights on from 0600 to 1800). Blood was obtained from fed (*open bars*) or fasted (*filled bars*) mice at 1000 h. Plasma levels of triglyceride (*panel A*), glucose (*panel B*), and ketone bodies (*panel C*) were measured as described under "Experimental Procedures." Results are presented as the mean ± S.D. from 12 mice in each group. The *asterisk* denotes statistical difference, $p < 0.01$.

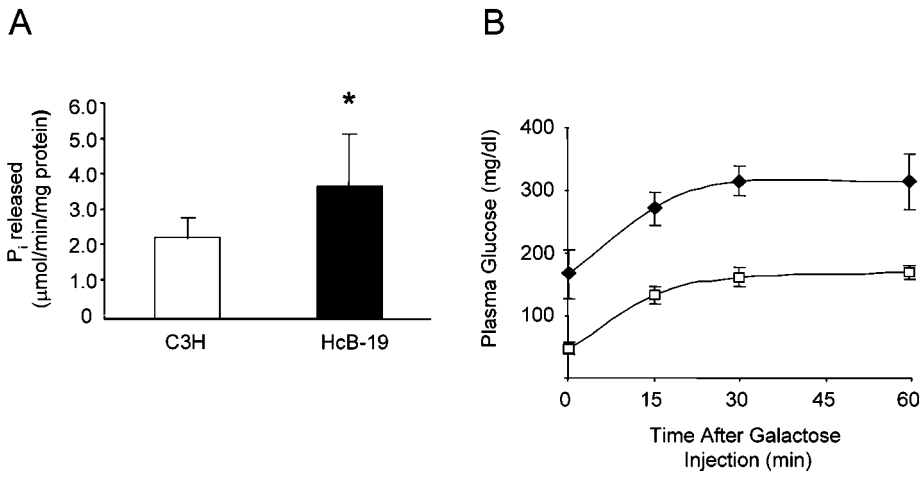

FIG. 2. **Comparison of G6Pase activities and abilities to utilize galactose in HcB-19 and control C3H mice.** *Panel A*, liver microsomes were prepared from overnight fasted C3H and HcB-19 mice. G6Pase activity was measured by following the amount of phosphate released over time and normalized to the amount of microsomal protein in each assay. Results are presented as mean ± S.D. from four mice in each group. The *asterisk* denotes statistical difference, $p < 0.05$. *Panel B*, galactose (3 g/kg of body weight in 0.9% saline) was injected (intraperitoneal) into fasting C3H (*filled diamonds*) and HcB-19 mice (*open squares*). Blood samples were collected by retro-orbital bleeding at 0, 15, 30, and 60 min after injection, and the amount of glucose was determined. Results are presented as the mean ± S.D. from five mice in each group.

first described as a model of human familial combined hyperlipidemia (12). The gene responsible for the HcB-19 phenotype is thioredoxin-interacting protein (Txnip) (13). A nonsense mutation renders the mice Txnip-null, which may enhance the activity of thioredoxin. Thioredoxin plays a role in buffering the redox state of proteins in which the standard redox potential ($E°$) of their disulfide bonds is within the physiological range (14–16). The HcB-19 mice, therefore, provide a new window into processes that are regulated by a redox rheostat.

EXPERIMENTAL PROCEDURES

Animals and Streptozotocin Treatment—HcB-19 and C3H/DiSnA mice derived from the colony at the University of California, Los Angeles (12, 13, 17, 18) were maintained under standardized conditions and fed with rodent chow 5015 and water *ad libitum*. The light-cycle hours were between 6 a.m. and 6 p.m. Streptozotocin (STZ) was injected intraperitoneally (50 mg/kg in 0.1 M sodium citrate buffer, pH 4.50) daily for 5 consecutive days. Control animals received the same volume of citrate buffer. Plasma glucose and triglyceride were assessed 21 days after the initial treatment.

Plasma Metabolites and Insulin Assays—Blood samples were collected from mice under isofluorane anesthesia in heparinized capillary tubes. Plasma was obtained by centrifugation at 12,000 × *g* for 5 min at 4 °C. Glucose and triglycerides in plasma were assayed with commercial kits from Sigma. Insulin and C-peptide were assayed using the ultra sensitive rat/mouse insulin RIA kit (Linco) and C-peptide RIA kit (Linco), respectively.

Glucose and Galactose Tolerance Tests—Glucose or galactose (3 g/kg of body weight in 0.9% saline) was injected (intraperitoneal) into fasting C3H and HcB-19 mice. Blood samples were collected by retro-orbital bleeding at 0, 15, 30, and 60 min after injection and centrifuged at 12,000 × *g* for 5 min at 4 °C. Glucose levels in the plasma were assayed with a commercial glucose diagnostic kit from Sigma.

Glucose 6-Phosphate (G6P) Phosphohydrolase Assays—Microsomes from overnight-fasted mice were thawed on ice and diluted with ice-cold 0.25 M sucrose solution to 30 ml/g of wet liver weight. The microsomal membrane was disrupted by the addition of 0.2% (w/v) sodium deoxycholate. Enzyme assays were carried out in 0.1 M sodium cacodylate buffer, pH 6.5, containing 20 mM G6P containing 100 μg of microsome protein per 0.75-ml reaction mixture. Incubations were at 30 °C for 10 min. The reactions were stopped by the addition of 0.5 ml of ice-cold trichloroacetic acid. Denatured protein was sedimented by centrifugation. Aliquots of the 200-μl supernatant fraction were assayed for inorganic phosphate by a colorimetric kit from Sigma.

Measurement of Gluconeogenic Intermediates in the Liver—Animals

were starved for 18 h before sacrifice. The livers were immediately removed and frozen in liquid nitrogen. The frozen tissue was ground in a porcelain mortar pre-cooled with liquid nitrogen. About 1 g of tissue powder was mixed with 5 ml of 0.6 M perchloric acid and centrifuged. The deproteinized supernatant fraction was removed and adjusted to pH 3.50 with 5 M potassium carbonate. Metabolites were estimated by standard spectrophotometric enzymatic assays as previously described (19, 20). G6P and fructose 6-phosphate (F6P) assays were carried out in 0.2 M triethanolamine buffer containing 0.2 mM NADP-Na_2 and 5 mM $MgCl_2$. Glucose-6-phospate dehydrogenase was then added, and the production of NADPH was monitored by following the absorbance at 339 nm. The amount of G6P in the samples was calculated from the amount of NADPH generated. After all G6P in the sample has been consumed, phosphoglucose mutase was added to convert F6P to G6P. The amount of F6P in the samples was estimated by the additional production of NADPH. Dihydroxyacetone phosphate (DHAP), glyceraldehyde 3-phosphate, and fructose-1,6-bisphosphate were assayed were sequentially in 0.2 M triethanolamine buffer containing 20 mM EDTA and 17 μM NADH. Glycerol-3-phosphate dehydrogenase was then added, and the conversion of NADH to NAD was followed by the change in absorbance at 339 nm. The amount of DHAP in the samples was calculated from the amount of NADH consumed. After the reaction has been completed, triose-phosphate isomerase was added to convert glyceraldehyde 3-phosphate into DHAP. The amount of glyceraldehyde 3-phosphate in the samples was estimated by the additional consumption of NADH. Finally, for the estimation of fructose-1,6-bisphosphate, aldolase was added to convert fructose-1,6-bisphosphate to DHAP and the change in NADH was measured.

Measurement of Glutathione Levels in the Liver—Glutathione levels in the liver were determined spectrophotometrically as described by Anderson (21). Briefly, mice were sacrificed and perfused with ice-cold PBS. Livers were excised and deproteinized with 10 volumes of 5% 5-sulfosalicylic acid. Total glutathione was determined using the 5,5′-dithiobis(2-nitrobenzoic acid)-GSSG reductase recycling assay. The production of 5-thio-2-nitrobenzoate was followed at 412 nm and is proportional to the amount of total glutathione in the sample. Oxidized glutathione was determined by the same assay after blocking the thiol group of GSH with 2-vinylpyridine.

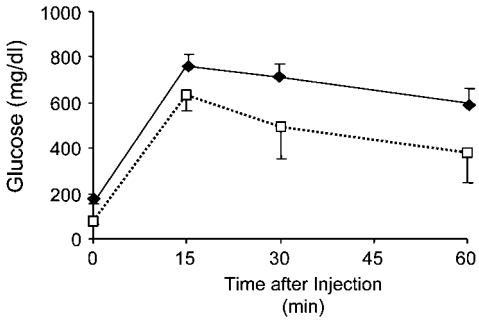

FIG. 3. **Glucose tolerance test.** Glucose (3 g/kg of body weight in 0.9% saline) was injected (intraperitoneal) into fasting C3H (*filled diamonds*) and HcB-19 mice (*open squares*). Blood samples were collected by retro-orbital bleeding at 0, 15, 30, and 60 min after injection, and the amount of glucose was determined. Results are presented as the mean ± S.D. from five mice in each group.

Quantitative Real-time PCR—Total RNA was isolated from the livers of mice by using the RNeasy mini kit (Qiagen). cDNA was synthesized using the Superscript First Strand Synthesis kit (Invitrogen) from 2 μg of total RNA (DNase I-treated) and random hexamer. Real-time PCR was performed in 96-well plates using the Bio-Rad iCycler machine. Typically, the 25-μl reaction contained 12.5 μl of 2xSYBR PCR Green Master Mix (Bio-Rad), 1 μl of cDNA, and 125 nM forward and reverse primers. All reactions were done in triplicate and optimized by melt curve analysis to ensure nonspecific products and primer dimers were not formed. The primer sequences used for SREBP-1a, SREBP-1c, SREBP-2, FAS, ACC, PEPCK, and apoB have been described (1, 22). ApoB mRNA was used as the invariant control. The relative amount of mRNA in each sample was determined by the comparative C_T method.

Statistical Analysis—Results are given as the mean ± S.D. Statistical significance was determined by two-tailed t test. Values of $p < 0.05$ were considered to be significant.

RESULTS

Loss of Txnip Is Associated with Fasting-induced Hypertriglyceridemia, Hypoglycemia, and Ketosis—As expected, overnight fasting caused triglycerides to decrease 3-fold in control mice (Fig. 1*A*). In striking contrast, plasma triglycerides increased 4-fold in HcB-19 mice in response to fasting (Fig. 1*A*). The fasting-induced hypertriglyceridemia uniquely displayed by HcB-19 mice is consistent with previous findings showing that the livers of HcB-19 mice secrete more VLDL particles (12, 13). However, the finding that HcB-19 mice showed no hyperlipidemia in the non-fasted state (Fig. 1*A*) suggests their metabolic disorder is distinct from familial combined hyperlipidemia proposed by earlier reports (12, 13).

Hepatic VLDL production rapidly adapts to nutritional status (23). Long term fasting is associated with decreased VLDL assembly and secretion (24, 25). The anomalous response to fasting by HcB-19 mice suggests that Txnip plays a role in eliciting the appropriate metabolic response to fasting.

Normal mice are able to maintain normal plasma glucose levels during fasting in part by stimulating hepatic gluconeogenesis. In contrast to the plasma glucose levels in excess of 100 mg/dl in control mice, HcB-19 mice became hypoglycemic (66.7 mg/dl) after a 14-h fast (Fig. 1*B*). Consistent with a previous report (12, 13), HcB-19 mice also showed a striking 6.6-fold increase in ketone bodies when fasted and a ~2-fold increase when fed (Fig. 1*C*).

Fasting-induced Hypertriglyceridemia and Hypoglycemia Associated with Loss of Txnip Are Not Caused by Defective Transport or Metabolism of Glucose 6-Phosphate—The fasting-induced hypoglycemia and hypertriglyceridemia phenotype of HcB-19 mice is similar to that of glycogen storage diseases caused by a deficiency in hepatic G6Pase and/or the glucose 6-phosphate transporter in the endoplasmic reticulum (26, 27). Our findings showing that hepatic microsomes from fasted HcB-19 mice contain higher levels of G6Pase activity than

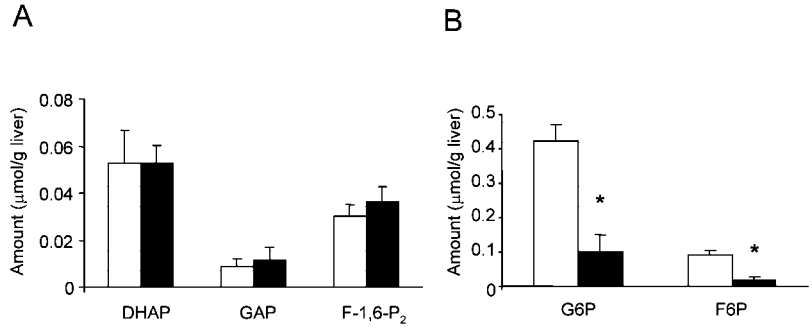

FIG. 4. **Steady-state levels of glycolytic/gluconeogenic intermediates in the livers of fasted HcB-19 and control C3H mice.** Hepatic contents of glycolytic/gluconeogenic intermediates in overnight-fasted control C3H (*open bars*) and HcB-19 (*filled bars*) mice were measured. *Panel A*, steady-state levels of DHAP, glyceraldehyde 3-phosphate (*GAP*), and fructose-1,6-bis-phosphate (*F-1,6-P2*). Results are presented as the mean ± S.D. from five mice in each group. *Panel B*, steady-state levels of G6P and F6P were assayed. Results are presented as the mean ± S.D. from five mice in each group. The *asterisk* denotes statistical difference, $p < 0.01$.

those from control mice (Fig. 2*A*) suggest that impaired G6Pase activity is not responsible for the fasting-induced hypertriglyceridemia, hypoglycemia, or ketosis associated with loss of Txnip.

We also determined how loss of Txnip affects the ability of liver *in vivo* to transport G6P into the lumen of the endoplasmic reticulum and export it as glucose. Galactose is selectively taken up by the liver for conversion to G6P, which can subsequently be used for the production of glucose for secretion into the bloodstream. This process requires an intact function of the G6Pase complex. Thus, the increase in plasma glucose after a bolus of galactose provides an estimation of the relative flux of substrate through G6Pase (28). As shown in Fig. 2*B*, injection of a bolus of galactose (3 g/kg of body weight, intraperitoneal) resulted in a similar increment in plasma glucose in both groups of mice. These findings indicate that the fasting-induced hypertriglyceridemia, hypoglycemia, and ketosis associated with loss of Txnip are not caused by defective transport or metabolism of G6P.

Fasting-induced Hypertriglyceridemia and Hypoglycemia Associated with Loss of Txnip Are Not Caused by Altered Rates of Removal of Glucose from Plasma—To examine the ability of each group of mice to remove glucose from plasma, fasted mice were challenged with a bolus of glucose (3 g/kg of body weight, intraperitoneal) (Fig. 3). Before glucose administration, HcB-19 mice exhibited lower plasma glucose levels that were ~50 mg/dl less than those of control mice (Fig. 3). Both groups exhibited similar net increments of plasma glucose as well as similar rates of removal of glucose from plasma after the bolus injection of glucose (Fig. 3). Thus, it appears that the fasting-induced hypoglycemia associated with loss of Txnip is not caused by accelerated removal of glucose from plasma and may be the result of decreased hepatic gluconeogenesis and glucose export.

Livers of Fasted HcB-19 Mice Display a Block Near the End Point of Hepatic Gluconeogenesis—To determine whether stimulation of hepatic gluconeogenesis is impaired in fasting HcB-19 mice, steady-state levels of glycolytic/gluconeogenic intermediates in the livers of fasted mice were measured (Fig. 4). Although the hepatic levels of fructose-1,6-bisphosphate (*F-1,6-P_2*) and triose phosphate intermediates (dihydroxyacetone phosphate and glyceraldehyde 3-phosphate) were similar in both groups, levels of G6P and F6P were markedly decreased in HcB-19 mice (>70%, $p < 0.01$) (Fig. 4). Together with the finding that HcB-19 mice can utilize G6P from galactose for glucose production (Fig. 2*B*), these data suggest that hypoglycemia is due to a lack of supply of G6P and F6P in the terminal steps of gluconeogenesis.

The reduction in G6P and F6P in the fasting HcB-19 livers could be due to decreased FBPase activity. The mRNA and protein levels of FBPase were similar in C3H and HcB-19 mice

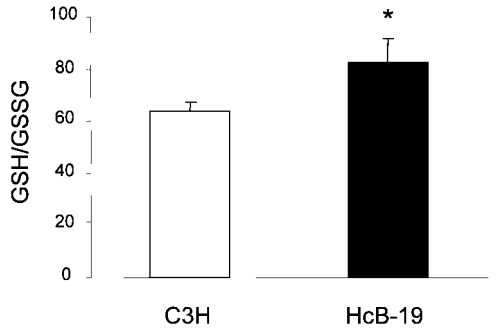

FIG. 5. **Sulfhydryl redox status in the livers of fasting HcB-19 and control C3H mice.** Levels of total GSH and GSSG were measured from perfused livers of overnight-fasted C3H (*open bars*) and HcB-19 (*filled bars*) mice. Results are presented as mean ± S.D. from five mice in each group. The *asterisk* denotes statistical difference, $p < 0.05$.

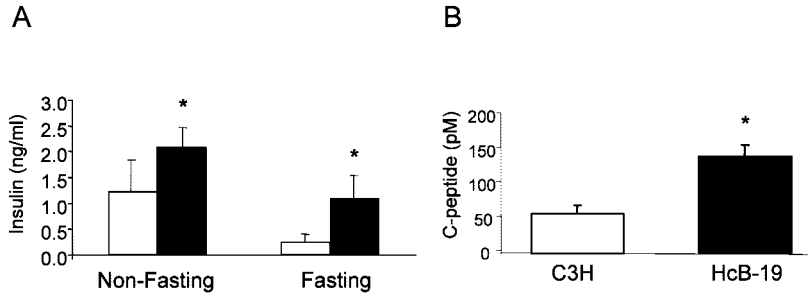

FIG. 6. **Plasma levels of insulin and C-peptide.** *Panel A*, plasma insulin levels. C3H (control) and HcB-19 were fed a chow diet and water *ad libitum* in a room with a 12-h light cycle (lights on from 0600 to 1800). Blood was obtained from fed (*open bars*) or fasted (*filled bars*) mice at 1000 h. Plasma levels of insulin were measured by RIA. *Panel B*, plasma C-peptide levels in fasting mice. Blood was obtained from fasting C3H (*open bars*) and HcB-19 (*filled bars*) mice at 1000 h. Plasma levels of C-peptide were measured by radioimmunoassay. Results are presented as the mean ± S.D. from six mice in each group. The *asterisk* denotes statistical difference, $p < 0.01$.

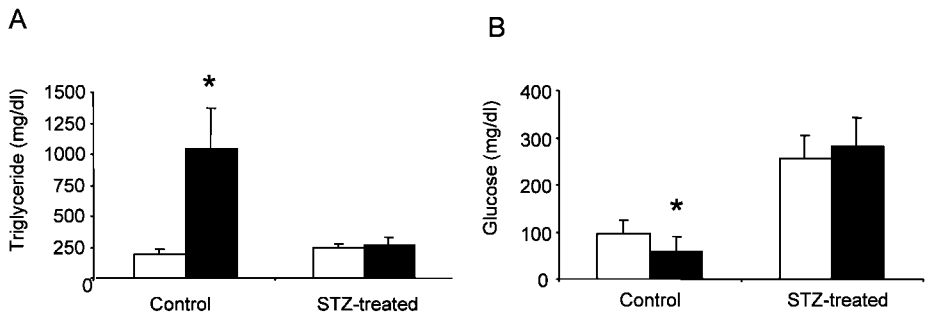

FIG. 7. **Effects of streptozotocin treatment on the hypertriglyceridemia and hypoglycemia phenotypes exhibited by fasted HcB-19 mice.** STZ was injected intraperitoneally (50 mg/kg in 0.1 M sodium citrate buffer, pH 4.50) daily for 5 days into C3H (*open bars*) and HcB-19 mice (*filled bars*). Control animals in each strain of mice received the same volume of citrate buffer. After 21 days, blood samples were collected from overnight-fasted mice in each group. Plasma levels of triglycerides (*panel A*) and glucose (*panel B*) were determined. Results are presented as the mean ± S.D. from five mice in each group. The *asterisk* denotes statistical difference, $p < 0.01$.

(Northern and Western blotting, data not shown), suggesting that the change in FBPase activity is due to post-translational modification and/or allosteric control.

Loss of Txnip Is Associated with Increased Thiol Redox (GSH/GSSG) Status, an Allosteric Regulator of Gluconeogenesis/Glycolysis—FBPase enzyme activity is negatively regulated by fructose 2,6-bisphosphate (5). This inhibition is exquisitely dependent upon the thiol (cysteine) redox state of the enzyme, the reduced form being more susceptible to the inhibition by fructose2,6-bisphosphate (29). Thus, gluconeogenesis and glycolysis are reciprocally responsive to the ratio of reduced glutathione:oxidized glutathione (GSH/GSSG) (30). A ~50% increase in the ratio of GSH/GSSG in renal tubules is associated with an up to 20-fold increased rate of gluconeogenesis (30). We, therefore, measured the GSH/GSSG ratio in the livers of both groups of fasted mice. In HcB-19 mice, the hepatic GSH/GSSG ratio was increased by 30% ($p < 0.05$) (Fig. 5). The 30% increased GSH/GSSG ratio in the liver displayed by HcB-19 mice is sufficient to account for the apparent block in FBPase observed in the livers of fasted HcB-19 mice (Fig. 4).

Loss of Txnip Is Associated with Increased Plasma Levels of Insulin and C-peptide—Because insulin suppresses gluconeogenesis and negatively regulates FBPase activity, we measured the plasma insulin levels in HcB-19 mice. As shown in Fig. 6*A*, plasma insulin concentrations were significantly elevated in both fed and fasting HcB-19 mice. In the fed state, plasma insulin levels in HcB-19 mice were about 50% higher than that of control. After an 18-h fast, the difference in plasma insulin levels between the 2 groups of mice was ~3-fold (Fig. 6*A*). Plasma C-peptide levels in fasted HcB-19 mice also showed a similar ~3-fold increase (Fig. 6*B*). These findings suggest that elevated plasma insulin levels in HcB-19 mice are linked to enhanced pancreatic β-cell secretion rather than reduced hepatic insulin clearance.

Livers from Fasted HcB-19 Mice Display a Selective Resistance to Hyperinsulinemia—Surprisingly, the hyperinsulinemia displayed by fasted HcB-19 mice was not associated with a detectable increase in the hepatic content of fructose 2,6-bisphosphate or reduced activity of fructose-1,6-bisphosphatase (data not shown).

Normally, insulin suppresses the expression of PEPCK. However, despite the 3-fold increase in insulin in fasted HcB-19 mice relative to normal mice, PEPCK expression in fasted HcB-19 mice was unchanged (*i.e.* not suppressed) compared with fasted controls (Table I). Interestingly, fed mice from both groups exhibited decreased expression of PEPCK mRNA and increased expression of lipogenic SREBP-1c, SREBP-2, ACC, and FAS compared with the levels displayed when fasted (Table I).

A second physiological function of PEPCK is glyceroneogenesis (2). The hyperlipidemic phenotype of the fasted HcB-19 mice would be consistent with an abnormally increased diversion of PEP toward glycerol production (via glycerol-3-phosphate dehydrogenase) and lipogenesis (31, 32). Consistent with increased lipogenesis, SREBP-1c levels in the fasted HcB-19 mice were 3.3-fold higher than those of control mice (Table I). As expected, the expression of SREBP-1c target genes, acetyl-CoA carboxylase, and fatty acid synthase were also increased 2-fold in fasted HcB-19 mice (Table I).

Because the changes in lipogenesis correlate with hyperinsulinemia, we ablated the insulin-producing β-cells of the normal and HcB-19 mice with STZ. In addition to the expected hyperglycemia associated with loss of insulin signaling, STZ treatment completely blocked the fasting-induced hypertriglyceridemia in the HcB-19 mice (Fig. 7). Thus, the fasting-induced hypertriglyceridemia of the HcB-19 mice is dependent upon insulin.

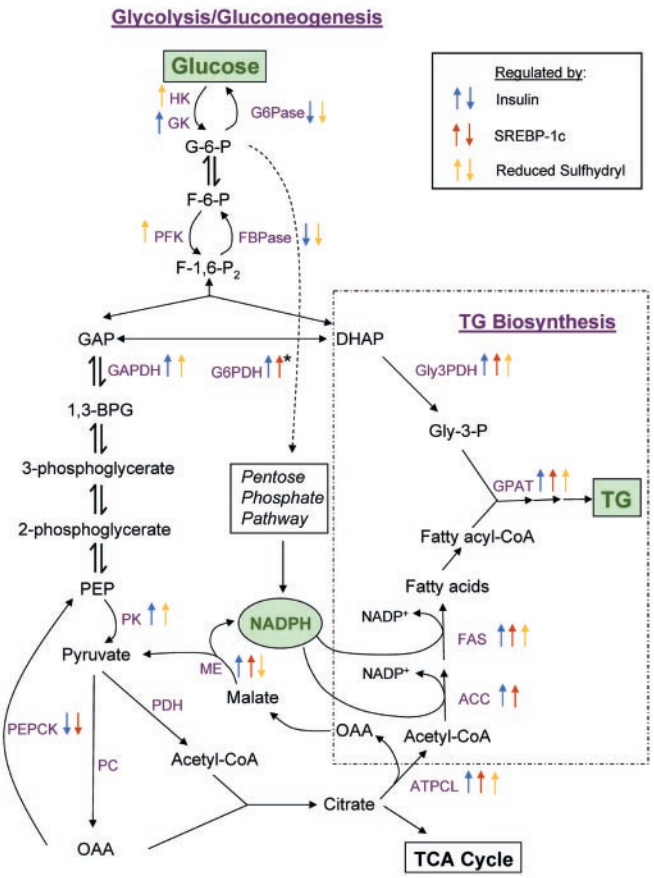

FIG. 8. **Regulation of glycolysis, gluconeogenesis, and triglyceride biosynthesis by insulin, SREBP-1c, and cellular sulfhydryl redox.** Activities of key enzymes in glycolysis, gluconeogenesis, and triglyceride (*TG*) synthesis are modulated by insulin (*blue arrows*), SREBP-1c (*red arrows*), and thiol redox status (*yellow arrows*). In the context of fasting HcB-19 mice with elevated plasma insulin, increased hepatic SREBP-1c mRNA expression combined with a greater reduced thiol redox status act in concert to activate enzymes in glycolysis and triglyceride biosynthesis and to reciprocally suppress gluconeogenic enzymes. Note that SREBP-1c is required to induce glucose-6-phosphate dehydrogenase in response to refeeding but is not required for expression in fasted mice (see Ref. 57). *TCA*, tricarboxylic acid; *HK*, hexokinase; *GK*, glucokinase; *PFK*, phosphofructokinase; *Gly3PDH*, glycerol-3-phosphate (*Gly-3-P*) dehydrogenase; *PDH*, pyruvate dehydrogenase; *ME*, malic enzyme; *ATPCL*, ATP:citrate lyase; *GPAT*, glycerol-3-phosphate acyltransferase; *OAA*, oxaloacetate; *1,3-BPG*, 1,3-bisphosphoglycerate; *PC*, pyruvate carboxylase; *GAP*, glyceraldehyde 3-phosphate.

DISCUSSION

Animals are able to reprogram their metabolic pathways to adapt to changes in nutrient availability, hormonal status, and energy demands. The mechanisms require sensing these stimuli and bringing about a change in the abundance or activation state of metabolic enzymes and regulators of gene expression. A recurring theme in metabolism is that cells sense their "energy charge" by responding to changes in ATP or AMP or to changes in "redox potential" as reflected in NAD(P)H/NAD+(P) and GSH/GSSG. The cysteine residues of many proteins exist in a dynamic state between the reduced free sulfhydryl and the oxidized disulfide bridge. There are many *in vivo* processes that allow redox potential to equilibrate NAD(P)H/NAD^+(P), GSH/GSSG, and protein sulfhydryl reduction/oxidation. The ubiquitous enzyme thioredoxin is mainly responsible for equilibrating NAD(P)H/NAD^+(P) redox potential with protein sulfhydryl redox state via the oxidation of NADPH (33–35). Thioredoxin function can itself be modulated by its interaction with its inhibitory protein partner, Txnip (36, 37). The availability of a

TABLE I

Quantitation of gene expression in C3H and HcB-19 mice by real-time PCR.

Livers were obtained at 1000 h (lights on from 0600 to 1800 h) from 12-week-old male C3H and HcB-19 mice that had been fasted for 18 h or were non-fasted. Total RNA and cDNA were prepared from these samples as described under "Experimental Procedures." Expression levels of mRNA relative to the constitutively expressed apoB mRNA are indicated and were determined by quantitative real-time PCR. Results from four mice in each group are presented as -fold increase relative to that of fasted C3H controls. Statistical differences were determined by Student's *t* test, and the two-tailed *p* values are listed.

	Relative mRNA expression levels					
	Fasted			Fed		
	C3H	HcB-19	*p* value (C3H *vs.* HcB-19)	C3H	HcB-19	*p* value (C3H *vs.*HcB-19)
	-Fold of increase vs. fasted C3H control					
SREBP-1a	1.00	1.62	0.183	1.19	1.04	0.790
SREBP-1c	1.00	3.28	0.012	11.44	9.46	0.308
SREBP-2	1.00	1.92	0.004	3.28	2.96	0.533
ACC	1.00	2.00	0.005	4.24	2.86	0.116
FAS	1.00	2.17	0.003	5.98	3.30	0.063
PEPCK	1.00	1.05	0.711	0.21	0.47	0.040

Txnip-null mutant mouse (13) provided an opportunity to discover the metabolic pathways that are affected by the loss of Txnip. This study establishes a causal connection between loss of Txnip resulting in enhanced sulfhydryl reduction and dysregulated carbohydrate and lipid metabolism. The work suggests that Txnip plays a role in at least two tissue sites, the liver and pancreatic β-cells.

To maintain homeostasis the liver must balance the flux of carbon units into gluconeogenesis with metabolic needs by sensing blood glucose and integrating this information with energy stores and redox state. Glucose sensing occurs both directly and through insulin. The discovery that SREBP-1c is an insulin target explained how hepatocytes modify the expression of enzymes in glycolysis and lipogenesis appropriate to the level of blood glucose (1, 38, 39).

In addition to blood glucose, cells respond to their own internal energy status. Fasting is associated with a more oxidized sulfhydryl redox state (40). Our results establish a connection between redox status, Txnip, and metabolic adaptation to fasting. Instead of becoming more glucogenic, the fasting liver of a Txnip-null mouse is lipogenic. The dearth of glucose leads to hypoglycemia and ketosis.

The fasted HcB-19 mice are hyperinsulinemic. Yet, they fail to suppress the expression of PEPCK. Together with the induction of SREBP-1c and its regulated genes, this presents a picture of selective insulin resistance analogous to those previously reported by Shimomura and co-workers (41) in lipodystrophic mice. PEPCK catalyzes the formation of PEP, a precursor for both glucose and glycerol production. In fasted HcB-19 mice, PEP is selectively channeled into glyceroneogenesis due to the block in FBPase (Fig. 4) and the increased demand for triglyceride synthesis caused by increased plasma levels of fatty acids observed in HcB-19 mice (12, 13) returning to the liver and increased hepatic synthesis due to increased expression of ACC and FAS (Table I).

Sulfhydryl redox state, as reflected by the ratio of cellular GSH/GSSG, reciprocally regulates enzymes involved in gluconeogenesis and glycolysis (for review, see Ref. 42) such as hepatic FBPase (gluconeogenesis) (43) and phosphofructokinase (glycolysis) (44). In addition, sulfhydryl redox state also modulates the activity of enzymes involved in fatty acid and glycerolipid biosynthesis such as ATP-citrate lyase (45, 46), FAS (47), glycerol-3-phosphate dehydrogenase (48), and glycerol-3-phosphate acyltransferase (49) (summarized in Fig. 8). The findings showing that GSH in the livers of fasted HcB-19 mice is 30% more reduced (Fig. 5) may explain the decreased flux of carbon units through FBPase and increased production of fatty acids and glycerolipids. As a result, carbon units are secreted as triglycerides as a component of VLDL (12, 13). The data showing increased hepatic content of mRNAs encoding the lipogenic transcription factor SREBP-1c and two of its transcriptional targets (ACC and FAS) (Table I) in fasted HcB-19 mice provides an additional mechanism through which insulin enhances the flow of carbon units from glucose export into hepatic VLDL secretion.

Our findings suggest a role for Txnip in the pancreatic β-cells. The increased insulin secretion in fasted HcB-19 mice could be due to increased secretion by individual β-cells or increased β-cells mass. We suspect the latter is more likely. Txnip has been shown to block the thioredoxin-sulfhydryl reduction by NADPH (36). This finding predicts that the absence of Txnip in HcB-19 mice would lead to increased thioredoxin reduction activity (50). Pancreatic β-cells contain abundant levels of thioredoxin (51), which may contribute to the intracellular processing and secretion of insulin (52). It is believed that thioredoxin facilitates the processing and maturation of insulin (36) and, thus, may prevent unfolded protein response-induced apoptosis of pancreatic β-cells (53, 54). Transgenic overexpression of thioredoxin in pancreatic β-cells protects mice from STZ-induced and autoimmune diabetes (51). Txnip-thioredoxin interactions may be an effective target for promoting insulin secretion without causing pancreatic β-cell apoptosis.

Glucose causes a large increase in Txnip expression in pancreatic β-cells (55) and in cultured fibroblasts (56). This response links nutritional state (*e.g.* glucose uptake) with redox state and subsequent metabolic regulation. Our findings further suggest that the cellular redox state provides a unifying parameter linking cellular response to nutritional state. This response is tuned via Txnip-mediated changes in sulfhydryl redox potential.

REFERENCES

1. Liang, G., Yang, J., Horton, J. D., Hammer, R. E., Goldstein, J. L., and Brown, M. S. (2002) *J. Biol. Chem.* **277,** 9520–9528
2. Reshef, L., Olswang, Y., Cassuto, H., Blum, B., Croniger, C. M., Kalhan, S. C., Tilghman, S. M., and Hanson, R. W. (2003) *J. Biol. Chem.* **278,** 30413–30416
3. Morris, M. D., Zilversmit, D. B., and Hintz, H. F. (1972) *J. Lipid Res.* **13,** 383–389
4. Hanson, R. W., and Reshef, L. (1997) *Annu. Rev. Biochem.* **66,** 581–611
5. Pilkis, S. J., Claus, T. H., Kurland, I. J., and Lange, A. J. (1995) *Annu. Rev. Biochem.* **64,** 799–835
6. Chou, J. Y. (2001) *Curr. Mol. Med.* **1,** 25–44
7. Wu, C., Okar, D. A., Newgard, C. B., and Lange, A. J. (2001) *J. Clin. Investig.* **107,** 91–98
8. Kissebah, A. H., Alfarsi, S., and Adams, P. W. (1981) *Metabolism* **30,** 856–868
9. Siri, P., Candela, N., Zhang, Y. L., Ko, C., Eusufzai, S., Ginsberg, H. N., and Huang, L. S. (2001) *J. Biol. Chem.* **276,** 46064–46072
10. Brunzell, J. D., Albers, J. J., Chait, A., Grundy, S. M., Groszek, E., and McDonald, G. B. (1983) *J. Lipid Res.* **24,** 147–155
11. Ito, Y., Azrolan, N., O'Connell, A., Walsh, A., and Breslow, J. L. (1990) *Science* **249,** 790–793
12. Castellani, L. W., Weinreb, A., Bodnar, J., Goto, A. M., Doolittle, M.,

Mehrabian, M., Demant, P., and Lusis, A. J. (1998) *Nat. Genet.* **18,** 374–377
13. Bodnar, J. S., Chatterjee, A., Castellani, L. W., Ross, D. A., Ohmen, J., Cavalcoli, J., Wu, C., Dains, K. M., Catanese, J., Chu, M., Sheth, S. S., Charugundla, K., Demant, P., West, D. B., de Jong, P., and Lusis, A. J. (2002) *Nat. Genet.* **30,** 110–116
14. Gething, M. J., and Sambrook, J. (1992) *Nature* **355,** 33–45
15. Follmann, H., and Haberlein, I. (1995) *Biofactors* **5,** 147–156
16. Arrigo, A. P. (1999) *Free Radic. Biol. Med.* **27,** 936–944
17. Demant, P., and Hart, A. A. (1986) *Immunogenetics* **24,** 416–422
18. Groot, P. C., Moen, C. J., Dietrich, W., Stoye, J. P., Lander, E. S., and Demant, P. (1992) *FASEB J.* **6,** 2826–2835
19. Gaja, G., Ragnotti, G., Cajone, F., and Bernelli-Zazzera, A. (1968) *Biochem. J.* **109,** 867–875
20. Clark, M. G., Bloxham, D. P., Holland, P. C., and Lardy, H. A. (1974) *J. Biol. Chem.* **249,** 279–290
21. Anderson, M. E. (1985) *Methods Enzymol.* **113,** 548–555
22. Yang, J., Goldstein, J. L., Hammer, R. E., Moon, Y. A., Brown, M. S., and Horton, J. D. (2001) *Proc. Natl. Acad. Sci. U. S. A.* **98,** 13607–13612
23. Davis, R. A. (1999) *Biochim. Biophys. Acta* **1440,** 1–31
24. Davis, R. A., Boogaerts, J. R., Borchardt, R. A., Malone-McNeal, M., and Archambault-Schexnayder, J. (1985) *J. Biol. Chem.* **260,** 14137–14144
25. Leighton, J. K., Joyner, J., Zamarripa, J., Deines, M., and Davis, R. A. (1990) *J. Lipid Res.* **31,** 1663–1668
26. Lei, K. J., Chen, H., Pan, C. J., Ward, J. M., Mosinger, B., Jr., Lee, E. J., Westphal, H., Mansfield, B. C., and Chou, J. Y. (1996) *Nat. Genet.* **13,** 203–209
27. Annabi, B., Hiraiwa, H., Mansfield, B. C., Lei, K. J., Ubagai, T., Polymeropoulos, M. H., Moses, S. W., Parvari, R., Hershkovitz, E., Mandel, H., Fryman, M., and Chou, J. Y. (1998) *Am. J. Hum. Genet.* **62,** 400–405
28. Hawkins, R. A., Kamath, K. R., Scott, H. M., and Burchell, A. (1995) *J. Inherited Metab. Dis.* **18,** 558–566
29. Reyes, A., Burgos, M. E., Hubert, E., and Slebe, J. C. (1987) *J. Biol. Chem.* **262,** 8451–8454
30. Winiarska, K., Drozak, J., Wegrzynowicz, M., Jagielski, A. K., and Bryla, J. (2003) *Metabolism* **52,** 739–746
31. Steinberg, D., Vaughan, M., Margolis, S., Price, H., and Pittman, R. (1961) *J. Biol. Chem.* **236,** 1631–1637
32. Spiegelman, B. M., and Green, H. (1981) *Cell* **24,** 503–510
33. Sen, C. K. (2000) *Curr. Top. Cell. Regul.* **36,** 1–30
34. Sheehan, D., Meade, G., Foley, V. M., and Dowd, C. A. (2001) *Biochem. J.* **360,** 1–16
35. Tanaka, T., Nakamura, H., Nishiyama, A., Hosoi, F., Masutani, H., Wada, H., and Yodoi, J. (2001) *Free Radic. Res.* **33,** 851–855
36. Nishiyama, A., Matsui, M., Iwata, S., Hirota, K., Masutani, H., Nakamura, H., Takagi, Y., Sono, H., Gon, Y., and Yodoi, J. (1999) *J. Biol. Chem.* **274,** 21645–21650
37. Nishiyama, A., Masutani, H., Nakamura, H., Nishinaka, Y., and Yodoi, J. (2001) *IUBMB Life* **52,** 29–33
38. Kim, J. B., and Spiegelman, B. M. (1996) *Genes Dev.* **10,** 1096–1107
39. Shimomura, I., Bashmakov, Y., Ikemoto, S., Horton, J. D., Brown, M. S., and Goldstein, J. L. (1999) *Proc. Natl. Acad. Sci. U. S. A.* **96,** 13656–13661
40. Isaacs, J., and Binkley, F. (1977) *Biochim. Biophys. Acta* **497,** 192–204
41. Shimomura, I., Hammer, R. E., Richardson, J. A., Ikemoto, S., Bashmakov, Y., Goldstein, J. L., and Brown, M. S. (1998) *Genes Dev.* **12,** 3182–3194
42. Gilbert, H. F. (1984) *Methods Enzymol.* **107,** 330–351
43. Pontremoli, S., Luppis, B., Traniello, S., Rippa, M., and Horecker, B. L. (1965) *Arch. Biochem. Biophys.* **112,** 7–15
44. Gilbert, H. F. (1982) *J. Biol. Chem.* **257,** 12086–12091
45. Cottam, G. L., and Srere, P. A. (1969) *Biochem. Biophys. Res. Commun.* **35,** 895–900
46. Osterlund, B. R., Packer, M. K., and Bridger, W. A. (1980) *Arch. Biochem. Biophys.* **205,** 489–498
47. Walters, D. W., and Gilbert, H. F. (1986) *J. Biol. Chem.* **261,** 13135–13143
48. Cho, Y. W., Kim, D., Park, E. H., and Lim, C. J. (2002) *Mol. Cell* **13,** 315–321
49. Jamdar, S. C., Soo, E., and Cao, W. F. (1998) *Biochim. Biophys. Acta* **1393,** 41–48
50. Junn, E., Han, S. H., Im, J. Y., Yang, Y., Cho, E. W., Um, H. D., Kim, D. K., Lee, K. W., Han, P. L., Rhee, S. G., and Choi, I. (2000) *J. Immunol.* **164,** 6287–6295
51. Hotta, M., Tashiro, F., Ikegami, H., Niwa, H., Ogihara, T., Yodoi, J., and Miyazaki, J. (1998) *J. Exp. Med.* **188,** 1445–1451
52. Taljedal, I. B. (1981) *Diabetologia* **21,** 1–17
53. Ron, D. (2002) *J. Clin. Investig.* **109,** 443–445
54. Kaufman, R. J. (2002) *J. Clin. Investig.* **110,** 1389–1398
55. Shalev, A., Pise-Masison, C. A., Radonovich, M., Hoffmann, S. C., Hirshberg, B., Brady, J. N., and Harlan, D. M. (2002) *Endocrinology* **143,** 3695–3698
56. Hirota, T., Okano, T., Kokame, K., Shirotani-Ikejima, H., Miyata, T., and Fukada, Y. (2002) *J. Biol. Chem.* **277,** 44244–44251
57. Horton, J. D., Shah, N. A., Warrington, J. A., Anderson, N. N., Park, S. W., Brown, M. S., and Goldstein, J. L. (2003) *Proc. Natl. Acad. Sci. U. S. A.* **100,** 12027–12032